INL/CON-08-14297
PREPRINT

Three-Dimensional Computational Fluid Dynamics Modeling of Solid Oxide Electrolysis Cells and Stacks

8th European SOFC Forum

Grant Hawkes
James O'Brien
Carl Stoots
Stephen Herring

July 2008

The INL is a
U.S. Department of Energy
National Laboratory
operated by
Battelle Energy Alliance

Three-Dimensional Computational Fluid Dynamics Modeling of Solid Oxide Electrolysis Cells and Stacks

Grant Hawkes, James O'Brien, Carl Stoots, Stephen Herring
Idaho National Laboratory
2525 Fremont MS 3870
Idaho Falls, Idaho 83415 USA
Tel: +1-208-526-8767
Grant.Hawkes@inl.gov

Abstract

A three-dimensional computational fluid dynamics (CFD) electrochemical model has been created for detailed analysis of a high-temperature electrolysis stack (solid oxide fuel cells operated as electrolyzers). Inlet and outlet plenum flow distributions are discussed. Maldistribution of plena flow show deviations in per-cell operating conditions due to non-uniformity of species concentrations. Models have also been created to simulate experimental conditions and for code validation. Comparisons between model predictions and experimental results are discussed.

Mass, momentum, energy, and species conservation and transport are provided via the core features of the commercial CFD code FLUENT. A solid-oxide fuel cell (SOFC) model adds the electrochemical reactions and loss mechanisms and computation of the electric field throughout the cell. The FLUENT SOFC user-defined subroutine was modified for this work to allow for operation in the electrolysis mode. Model results provide detailed profiles of temperature, Nernst potential, operating potential, activation over-potential, anode-side gas composition, cathode-side gas composition, current density and hydrogen production over a range of stack operating conditions. Variations in flow distribution, and species concentration are discussed. End effects of flow and per-cell voltage are also considered. Predicted mean outlet hydrogen and steam concentrations vary linearly with current density, as expected. Contour plots of local electrolyte temperature, current density, and Nernst potential indicate the effects of heat transfer, reaction cooling/heating, and change in local gas composition.

Introduction

A research program is under way at the Idaho National Laboratory (INL) to simultaneously address the research and scale-up issues associated with the implementation of planar solid-oxide electrolysis cell technology for hydrogen production from steam. The research program includes an experimental program aimed at performance characterization of electrolysis cells and stacks. Results of some multi-cell tests have been documented in several recent papers [1], [2]. This paper reports the continued plenum study of a 60 cell stack when modeling a planar solid oxide electrolysis cells (SOEC) with the FLUENT code and SOFC module [3]. This model is similar to the one reported in Reference [4]. This model has a smaller permeability in the porous media than [4]. This code was used for detailed SOEC modeling. Fluent Inc. was funded by the US Department of Energy National Energy Technology Laboratory (DOE-NETL) to develop a solid-oxide fuel cell (SOFC) module for coupling to the core mass, momentum, energy, and species

conservation and transport features of the FLUENT CFD code. The SOFC module adds the electrochemical reactions and loss mechanisms and computation of the electric field throughout the cell. The FLUENT SOFC user-defined subroutine was modified for this work to allow for operation in the SOEC mode. Model results provide detailed profiles of temperature, Nernst potential, operating potential, anode-side gas composition, cathode-side gas composition, current density and hydrogen production over a range of stack operating conditions. Reference [5] has details of the FLUENT code and numerical model of a single electrolysis cell. Results of the numerical model are shown in this paper.

Numerical Model

The numerical model developed for this paper was based on the geometry of a 60 cell stack fabricated by Ceramatec, Inc. and tested at the INL. A depiction of four 60-cell stacks comprising an integrated lab scale (ILS) [6] module is shown in Figure 1. The stack has a per-cell active area of 64 cm^2. It is designed to operate in cross flow, with the steam/hydrogen gas mixture entering the inlet manifold on the right/front in the depiction, and exiting through the outlet manifold located in the center. Air flow enters at the other center manifold (not visible in Fig. 1) and exits at the front/left where the tabs are shown directly into the furnace. The power lead attachment tabs, integral with the upper and lower interconnect plates are also visible in the depiction, but not included in the model. Figure 2 shows the piping for the H2/H2O inlet and outlet and air inlet. Figure 3 shows the H2/H2O and air inlet pipes and inlet plena. Air is depicted as pink in this figure, with the H2/H2O plenum green. The figure has transparency turned on to be able to see the cell as it is depicted forward. Figure 3b shows the air and H2/H2o flow channels (current collectors) added. Figure 3c adds the outlet plena for the air and H2/H2O.

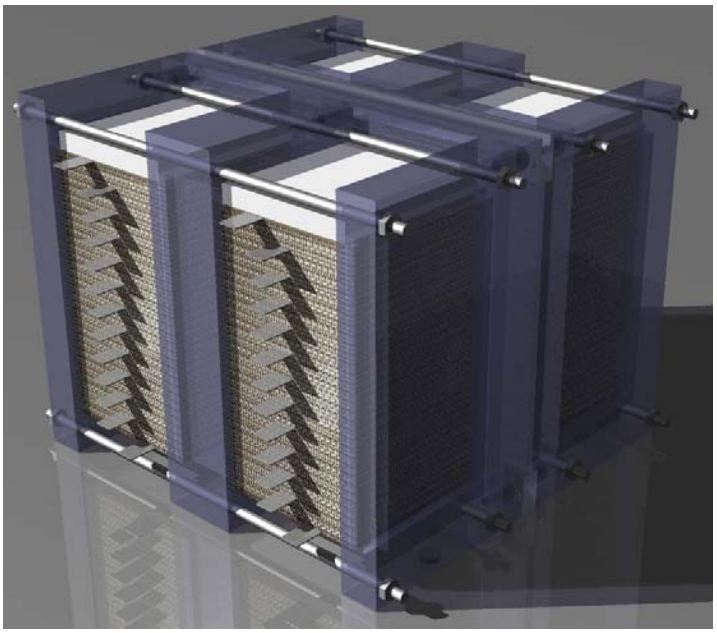

Figure 1. Depiction of ILS module with four 60-cell stacks.

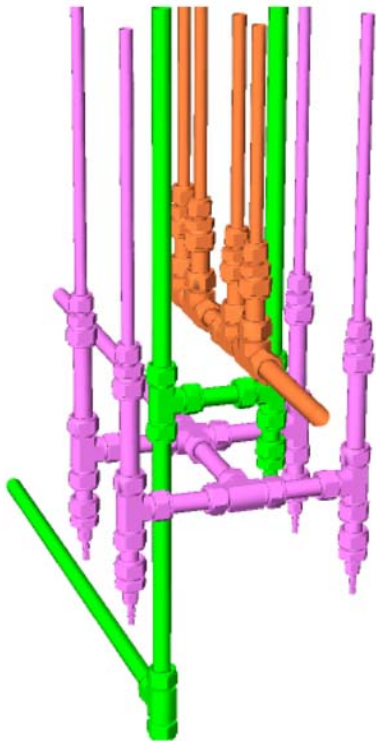

Figure 2. Inlet and outlet piping maze. Green = air inlet, pink = H2/H2O inlet, orange = H2 outlet.

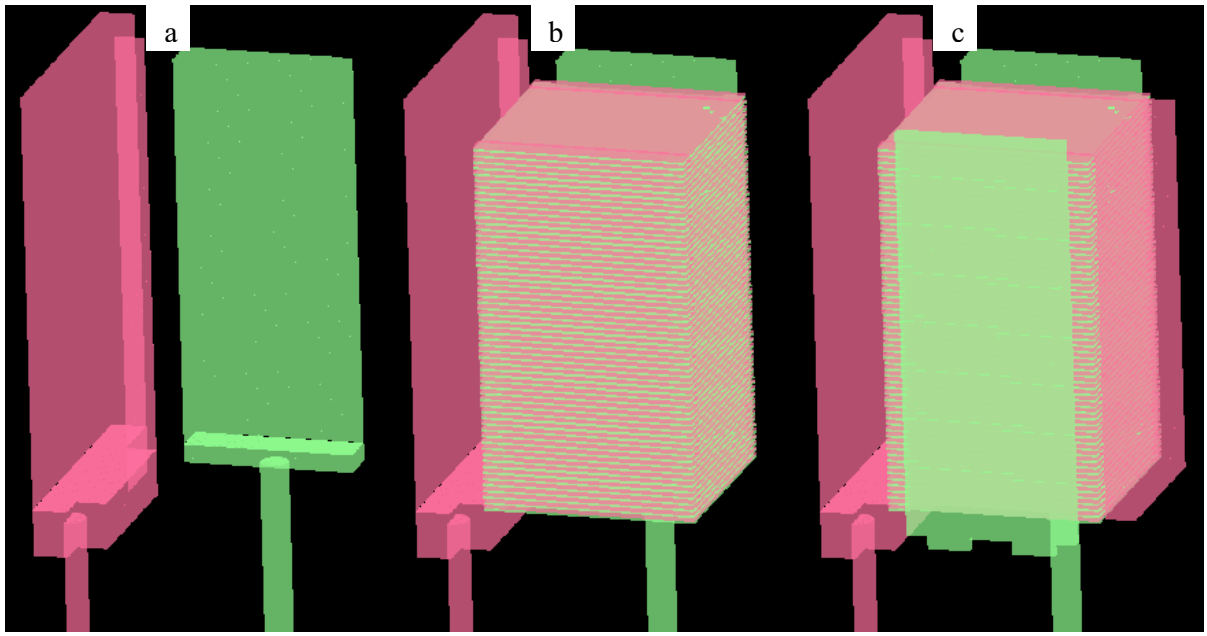

Figure 3. (a) Air (pink) and H2O/H2 (green) inlet pipe and inlet plenum, (b) with current collectorsadded, (c) with outlet plena added.

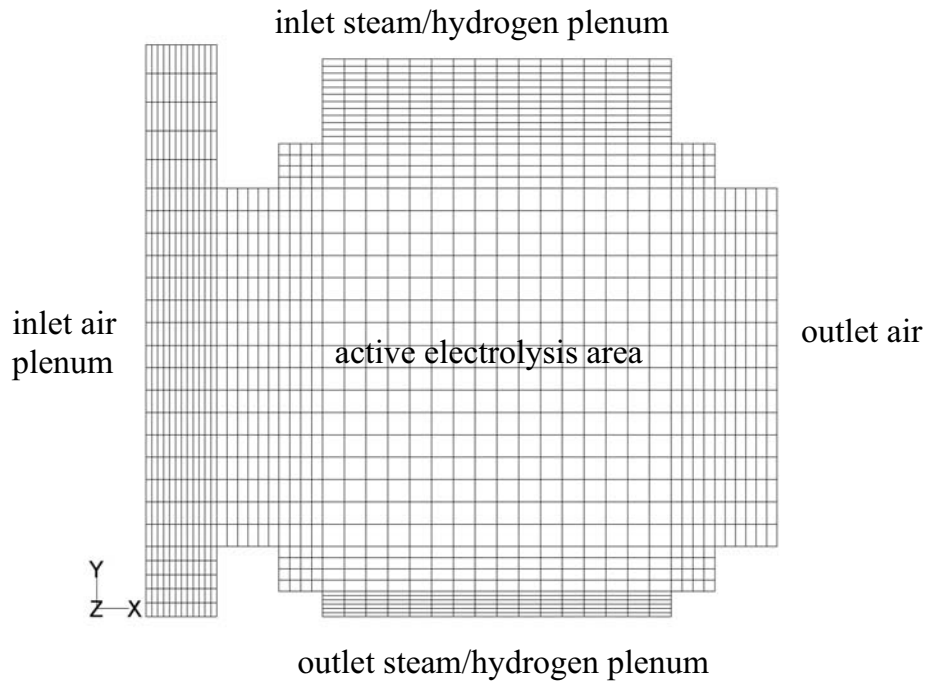

Figure 4. Mesh used in electrolytic area.

The numerical model geometry represents a complete 60 cell stack that is ¼ of the ILS module. Symmetry boundary conditions are implemented. The numerical domain extends from the bottom of the inlet tubes to the outlet flow path of each stream. Inlet flow tubes for the H2/H2O and air side are modeled 5-in. below the inlet of the plenum. This distance allows the flow to develop.

The FLUENT SOFC module treats the electrolyte as a 2-D planar element. Therefore the electrolyte in the model has geometrical thickness of zero. The electrolyte in the stack has a thickness of 0.14 mm. This thickness was apportioned to the separator plates so as to keep the total stack height correct. On either side of the electrolyte are the electrodes that are created with 3-D elements. Therefore, the electrolyte/electrode assembly in the model is only as thick as the two electrodes. Heat and mass sources and sinks are applied to the electrodes adjacent to the electrolyte via the FLUENT SOFC module.

Approximately 1.5 million elements are included in this model. Figure 4 shows the top view of the grid used. This grid was used at each level throughout the entire height of the model. The numerical grid used in this study included 4 elements each in the flow inlet and outlet regions, and 16 x 16 in the active cell area in the X and Y directions. Each flow channel (current collector) has 6 elements across the flow channel. Single cell numerical models with these numbers of cells give identical results to twice as many, meaning that the model is grid converged in the cell area. More research needs to be done on the mesh in the inlet and outlet plenum areas. Figure 5 shows a blown up view of a single cell with its components that are scaled 10x in the z-direction.

All external surfaces are considered to be adiabatic. This is certainly an accurate boundary condition for the symmetry conditions interior to the ILS module. Previous models have considered radiation heat transfer on the outer surface. The purpose of this model was to discover the flow uniformity and performance of a 60 cell stack. Details of the core mass, momentum, energy, and species conservation and transport features of FLUENT are documented in detail in the FLUENT user manual from Fluent Inc. Details of the electrochemical reactions, loss mechanisms, electric field computation, and electrode porous media constitutive relations are documented by the SOFC module in the FLUENT documentation. This reference also documents the treatment of species and energy sources and sinks arising from the electrochemistry at the electrode-electrolyte interfaces.

A mass flow rate of 2.18 x 10^{-4} kg/s and 1.83 x 10^{-4} kg/s were implemented as boundary conditions at the H2/H2O and air inlets respectively. Mole fractions of 0.10 and 0.90 for H2 and H2O respectively were set at the H2/H2O inlet. Electrical conductivity, tortuosity, exchange current density, and other parameters were taken from the base case of Reference [7].

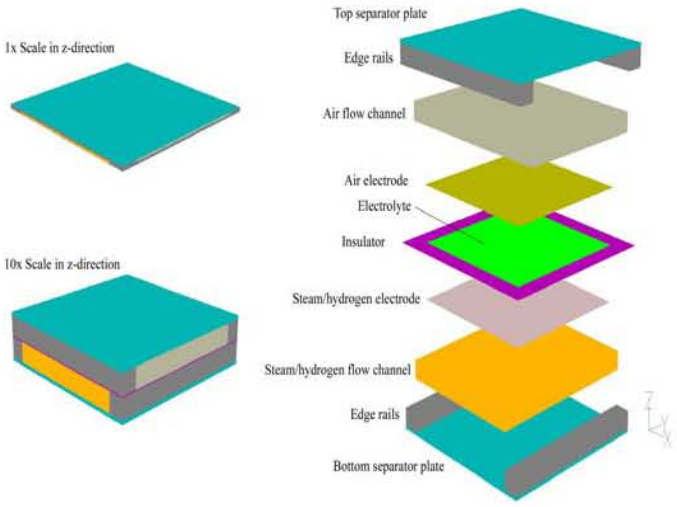

Figure 5. Component description for a single cell.

Results

Results are displayed on Figures 6 through 16. Figure 6 shows the path lines of the flow for the air inlet and H2/H2O inlet at open cell voltage (OCV) respectively. Most of the flow appears to go all the way to the top of the plenum and then recirculate down the outside before entering into each cell. Figure 7 shows the voltage versus current curve for this stack and operating conditions. A concave-down curve is typical for these planar cross-flow electrolyzers with adiabatic boundary conditions.

Figure 8 shows the temperature versus voltage curve for the four points modeled for this paper. As discussed in References [4] and [7], an operating voltage at 1.287 V/cell for an inlet gas temperature of 1073 K is known as the thermal neutral voltage. This point occurs where the endothermicity of the reaction splitting H2O is equal to the heat generated with Ohmic heating in the cells and stack. The outlet gas temperatures must be equal to the inlet gas temperatures at this point. This point corresponds to 77.2 V for the 60 cell stack. This model predicts with 0.01 degrees this correct mass flow rate weighted average exit gas temperature. Shown in Figure 9 are temperature contour plots displayed on every tenth electrolyte for open cell voltage (OCV), 60 V, 68 V, and 77.2 V. For all figures, the H2/H2O inlet is at the back right, while the air inlet is at the back left. Each contour plot has it own color bar legend that ranges from the minimum to the maximum in the model. These values correspond to 1.0, 1.13, and 1.28667 V/cell respectively. The second and third figures are dominated by the endothermic reaction and show temperatures well below the inlet conditions, while the fourth figure has a mean outlet gas temperature exactly equal to the inlet temperature of 1073 K.

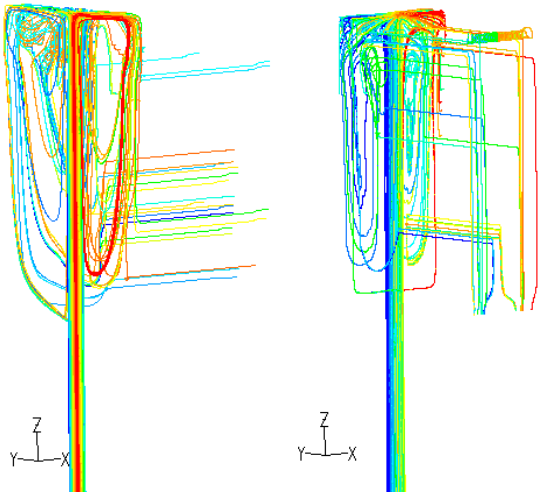

Figure 6. Pathlines for O2 (left) and H2/H2O (right)

Figure 10 shows the Nernst potential on each tenth electrolyte for the same four operating voltages. Nernst potential depends on the gas compositions and temperature. The temperature is dependent on the current density because of the endothermicity of the reaction. The fourth figure shown in Figure 10 has the same temperatures as the first, but the Nernst potential is dominated by the change in mole fractions because of the large amount of H2 and O2 produced and H2O consumed. Figure 11 shows the current density on each tenth electrolyte in the stack. The highest magnitude of current density and hence H2 production are the most negative. This high current density region always occurs at the H2/H2O inlet since it has the most favorable Nernst potential due to the species

concentrations. Shown in Figure 12 are the voltages at each separator plate. The colors are all the same because the scales are different for each figure going from ground (0V) to the boundary condition set at the current collector of 60V, 68V, and 77.2V respectively. Figure 13 shows the H2 mole fraction in the H2/H2O inlet plenum, H2 current collector, and the surface on the outlet of the H2/H2O outlet plenum. All four figures have the same scale in the legend. The second and third figures of Figure 13 show a slight increase in H2 concentration near the air inlet side. Once again, the most hydrogen is produced at the corner where the current density is the highest or where the species concentrations are the most favorable for the Nernst equation. For the thermal neutral case in the fourth figure of Figure 13, the H2 is evenly produced about throughout the height of the stack.
Shown in Figure 14 is the O2 mole fraction displayed on the O2 current collector, and air inlet plenum and inlet pipe. The amount of O2 produced is higher near the H2/H2O inlet side. This is due to the high concentration of H2O available to be electrolyzed as shown by the Nernst potential.

Figure 15 shows the per cell mass flow rate exiting each cell for the H2/H2O side for various permeability values in the current collector. Viscosity values varying with temperature were implemented with the ideal-gas-mixing-law choice in FLUENT. The base case used in all models has an inverse permeability in the current collector of 25×10^6 $1/m^2$. This value was calculated using Darcy flow through the thin flow channels. A permeability value was found where the pressure drop (~12 Pa) in the porous media modeled current collector was equal to the pressure drop through the thin rectangular channel with frictional flow. To find out the variation in flow through the cell, a value of 10x and 1/10x was used to show the flow distribution for the OCV case. The base case has flows varying less than one percent, while the least resistive case shows quite a maldistributed flow through the cells. The higher resistive case has a nearly uniform flow.
Shown in Figure 16 are the per-cell mass flow rates exiting from each cell on the H2/H2O side. Mass is being transported to the air side through the production of O2 as the voltage or current increases in each different case. There is a slight increase in flow near the bottom of the model. This is possibly due to the Venturi affect on the outlet side where all the flow passes through the two small outlet tubes.

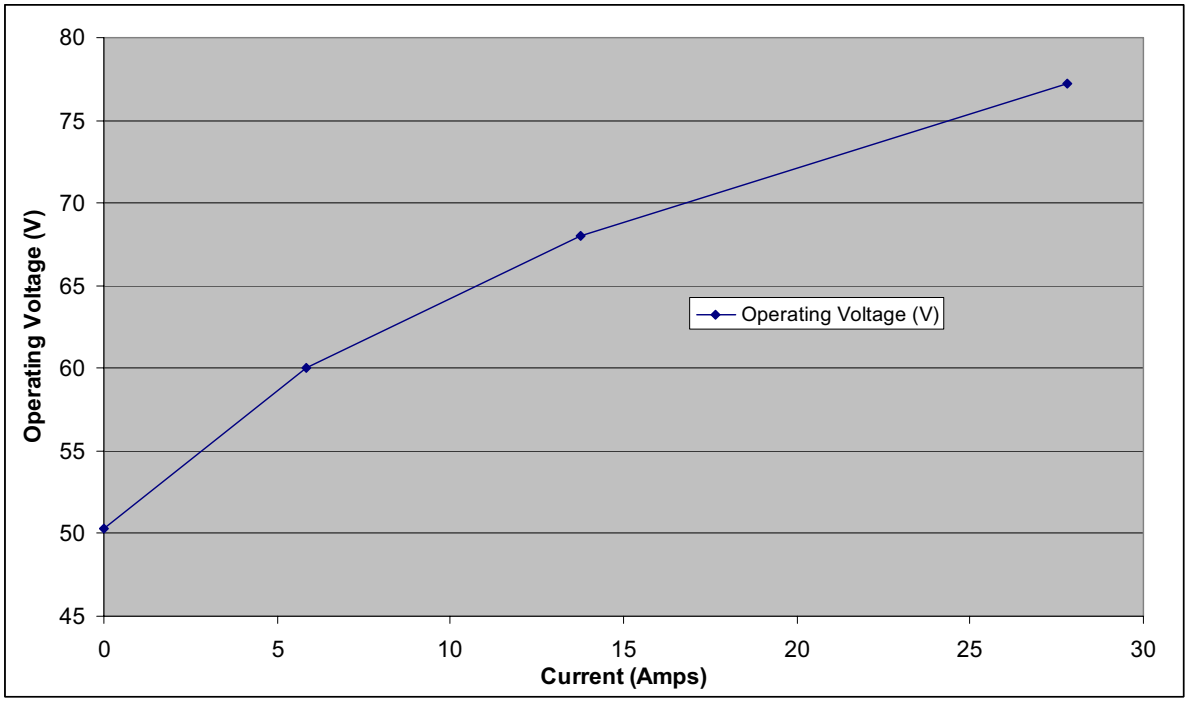

Figure 7. Operating voltage versus current for 60-cell stack.

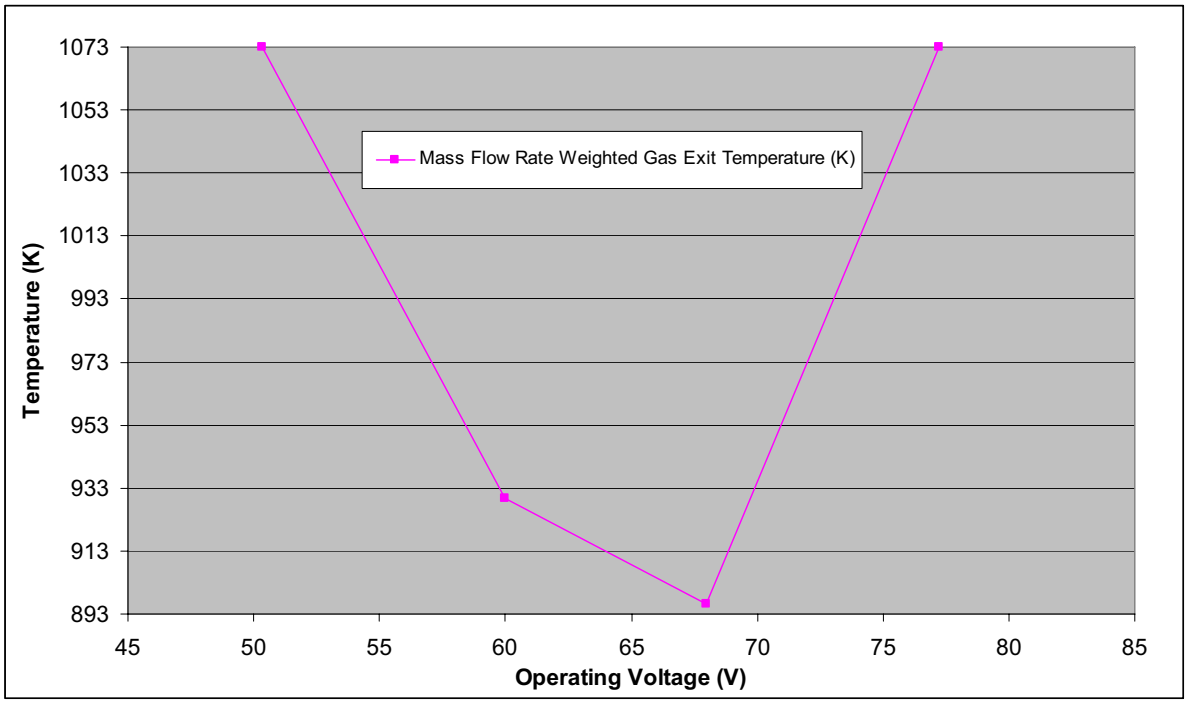

Figure 8. Temperature versus operating voltage for 60-cell stack.

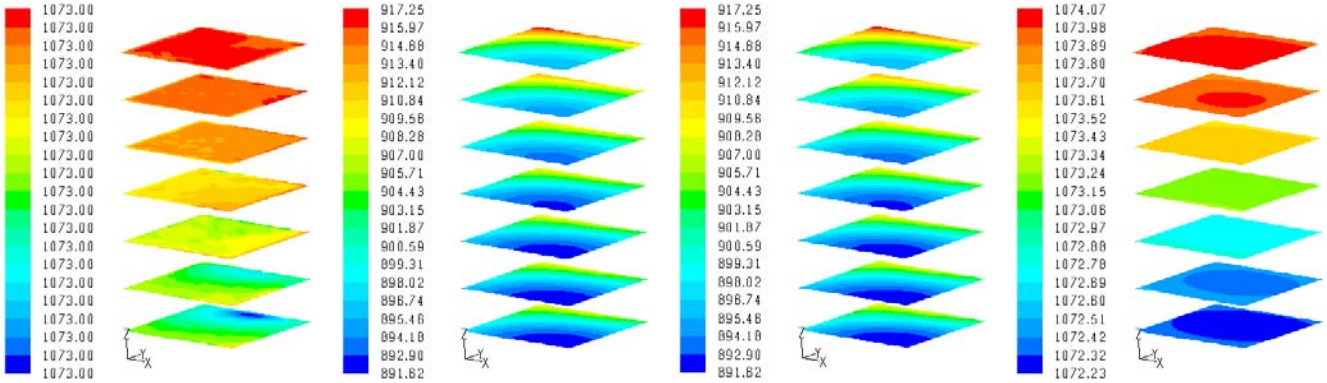

Figure 9. Temperature (K) contours plotted on every tenth electrolyte for OCV, 60V, 68V, and 77.2V.

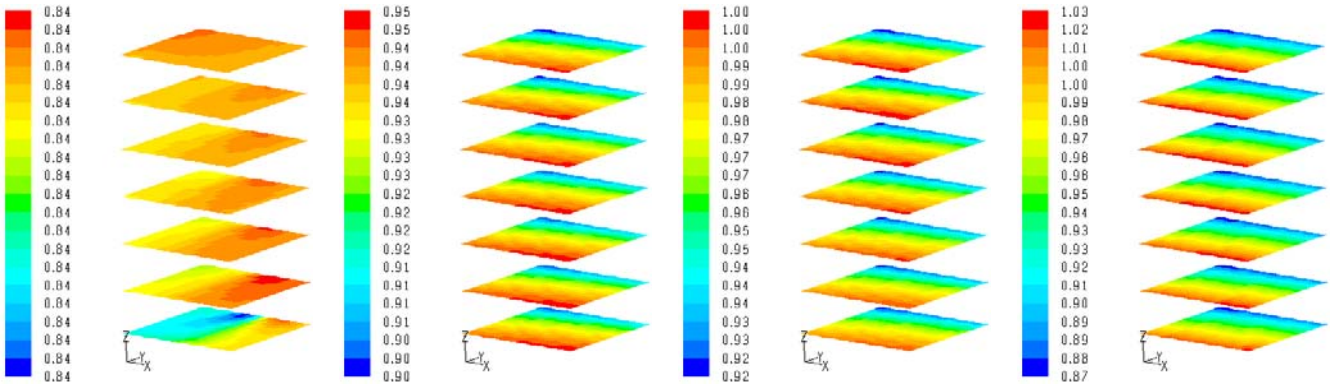

Figure 10. Nernst potential (V) contours plotted for every tenth electrolyte for OCV, 60V, 68V, and 77.2V.

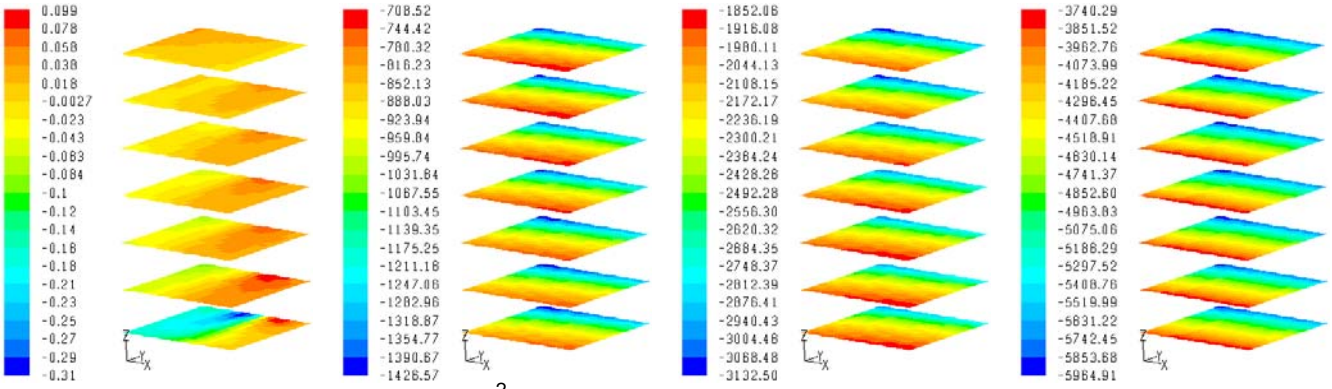

Figure 11. Current density (A/m^2) for OCV, 60V, 68V, and 77.2V.

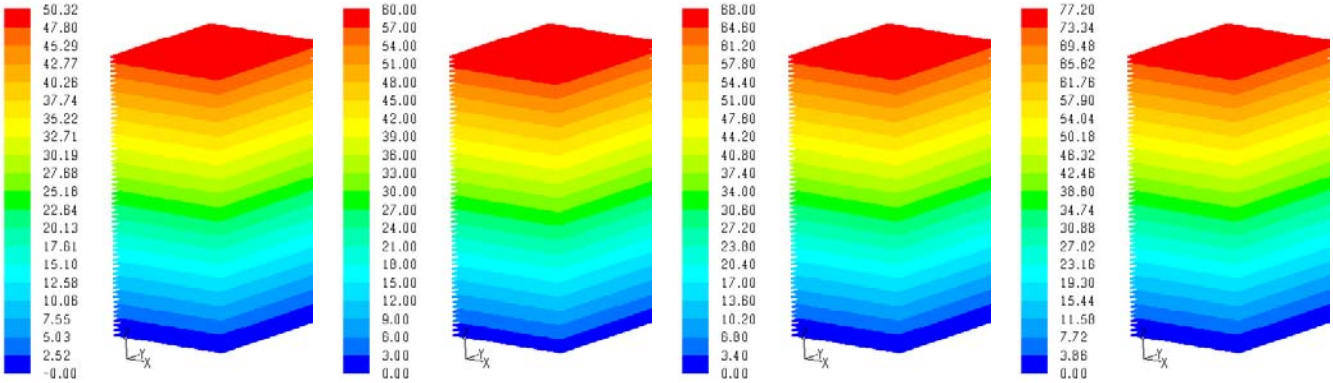

Figure 12. Operating voltage (V) for OCV, 60V, 68V, and 77.2V.

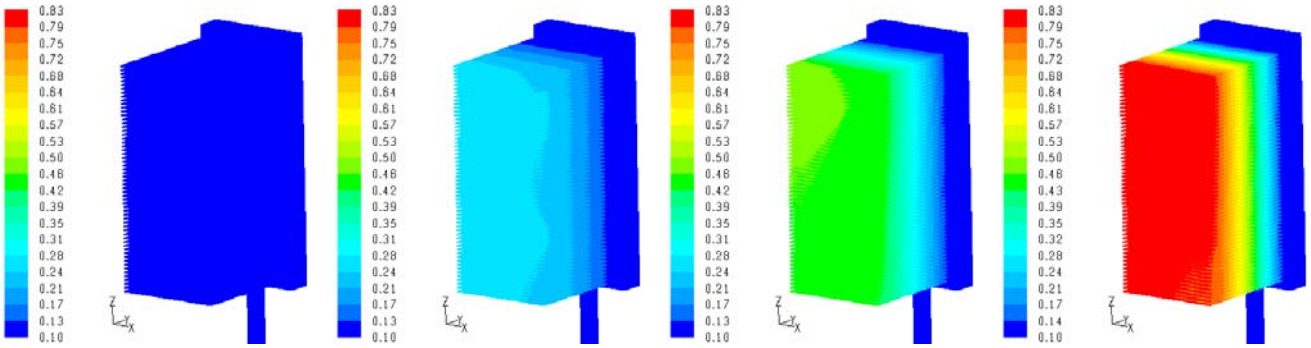

Figure 13. H2 mole fraction for OCV, 60V, 68V, and 77.2V.

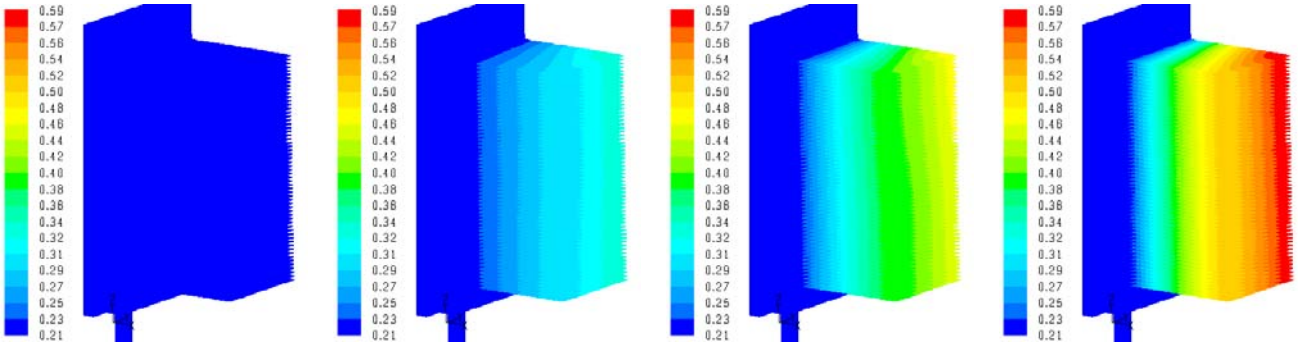

Figure 14. O2 mole fraction for OCV, 60V, 68V, and 77.2V.

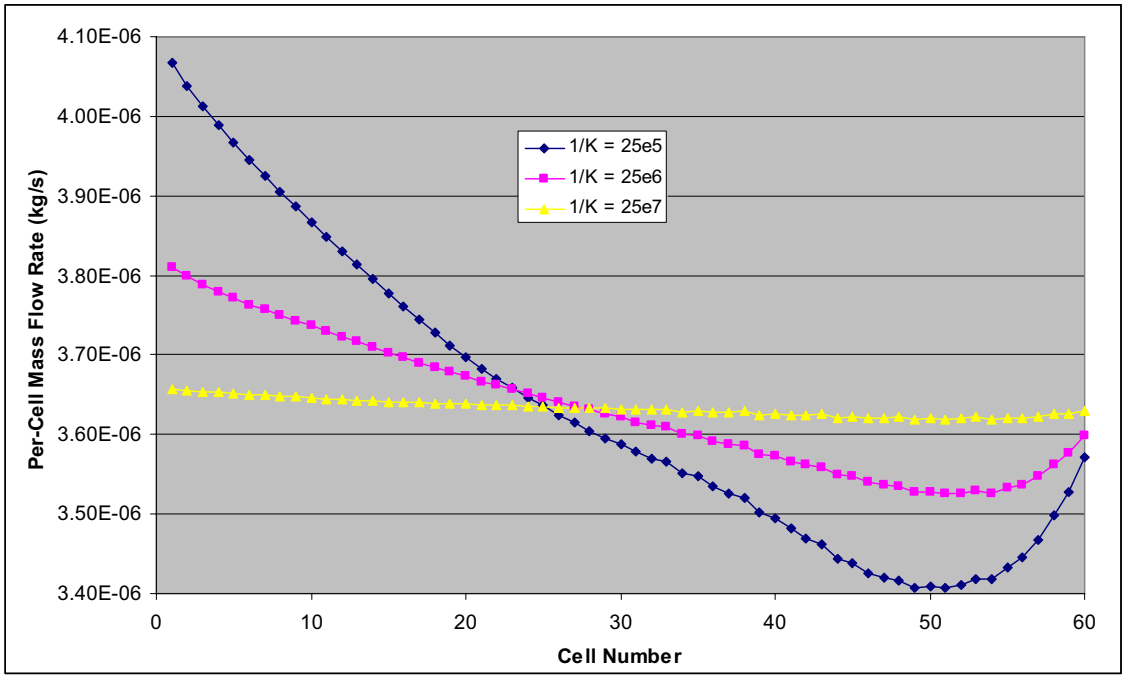

Figure 15. Mass flow rate exiting per cell for H2/H2O varying with permeability.

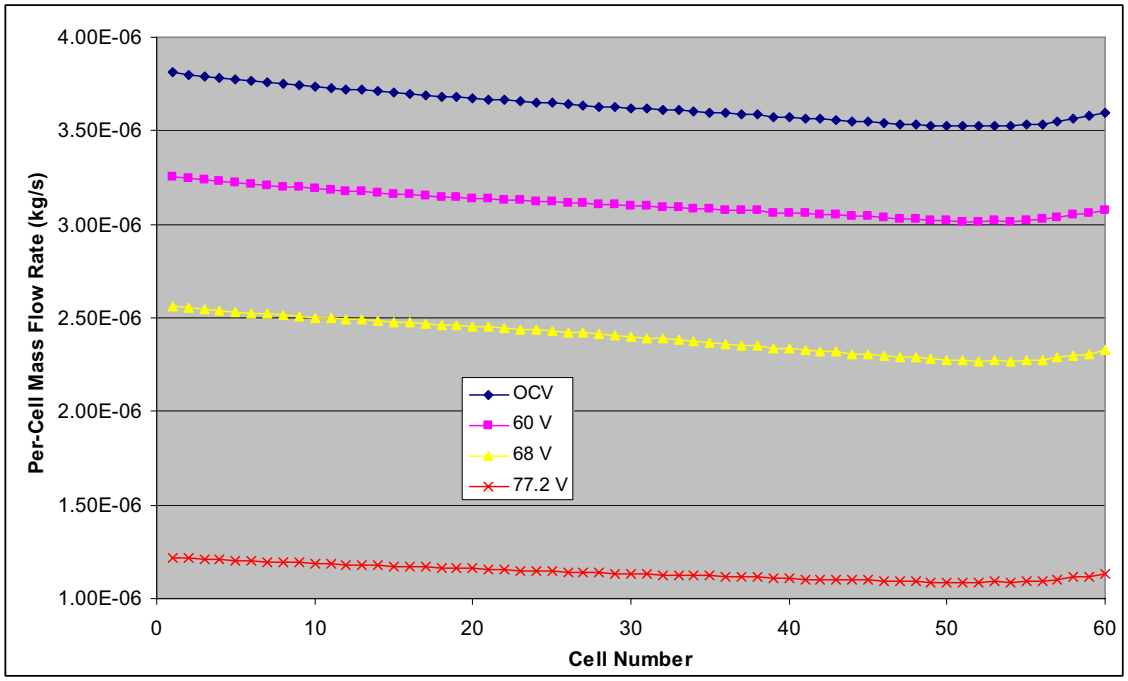

Figure 16. Mass flow rate exiting per cell for H2/H2O varying with voltage.

Conclusions

A three-dimensional computational fluid dynamics (CFD) model has been created to model high-temperature steam electrolysis in a planar solid oxide electrolysis cell (SOEC) stack. Effects of the variation of input parameters are shown for this stack and model. The model represents 60-cell stack that represents a ¼ of an ILS module. Details of the model geometry are specific to a stack that was fabricated by Ceramatec, Inc. and tested at the

Idaho National Laboratory. Mass, momentum, energy, and species conservation and transport are provided via the core features of the commercial CFD code FLUENT. A solid-oxide fuel cell (SOFC) model adds the electrochemical reactions and loss mechanisms and computation of the electric field throughout the cell. The FLUENT SOFC user-defined subroutine was modified for this work to allow for operation in the SOEC mode. Model results provide detailed profiles of temperature, Nernst potential, operating potential, anode-side gas composition, cathode-side gas composition, current density and hydrogen production over a range of stack operating conditions. Inlet and outlet plenums are included in the model of this stack. Plenum flow characteristics with recirculation were observed. Contour plots of local electrolyte temperature, current density, and Nernst potential indicated the effects of heat transfer, reaction cooling/heating, and change in local gas composition.

Mass flow rates vary less than one percent between various cells in the stack. A study of current collector permeability shows a pressure drop of ~12Pa pressure drop through the current collectors for the base case.

Acknowledgements

The U.S. Department of Energy, Office of Nuclear Energy, Nuclear Hydrogen Initiative Program supported this work. The DOE National Energy Technology Laboratory (NETL) provided the SOFC module to the INL for this research. The Idaho National Laboratory is operated by the Battelle Energy Alliance through DOE Contract DE-AC07-05ID14517.

References

[1] J. E. O'Brien, C. M. Stoots, J. S. Herring, and J. J. Hartvigsen, "Performance of Planar High-Temperature Electrolysis Stacks for Hydrogen Production from Nuclear Energy," *Nuclear Technology*, Vol. 158, pp. 118 - 131, May, 2007.

[2] J. E. O'Brien, C. M. Stoots, J. S. Herring, and J. J. Hartvigsen, "Hydrogen Production Performance of a 10-Cell Planar Solid-Oxide Electrolysis Stack," *Journal of Fuel Cell Science and Technology*, Vol. 3, pp. 213-219, May, 2006.

[3] Prinkey, M., Shahnam, M., and Rogers, W. A., "SOFC FLUENT Model Theory Guide and User Manual," Release Version 1.0, FLUENT, Inc., 2004.

[4] G. L. Hawkes, J. E. O'Brien, and C. M. Stoots, "3D CFD Model of a Multi-Cell High Temperature Electrolysis Stack, paper # 412d, 2007 AIChE Annual Meeting, Salt Lake City, November 4 – 9, 2007

[5] G. L. Hawkes, J. E. O'Brien, C. M. Stoots, J. S. Herring, "CFD Model of a Planar Solid Oxide Electrolysis Cell for Hydrogen Production from Nuclear Energy," *Nuclear Technology*, Vol. 158, pp. 132 - 144, May, 2007.

[6] C. M. Stoots, J. E. O'Brien, "Initial Operation of the High-Temperature Electrolysis Integrated Laboratory Scale Experiment at INL," 2008 International Congress on Advances in Nuclear Power Plants, June 8-12, 2008, Anaheim, CA

[7] G. L. Hawkes, R. W. Jones, "CFD Model of a Planar Solid Oxide Electrolysis Cell: Base Case and Variations," 2007 ASME-JSME Thermal Engineering Conference and Summer Heat Transfer Conference, July 8 – 12, 2007, Vancouver, BC, Canada.